

## Dissolution and Melting of Constituent Particles in a DC-cast Al-Zn-Mg-Cu Alloy 7150 During Homogenisation

Hua Chen<sup>1</sup>, Sam X. Gao<sup>2</sup>, Paul A. Rometsch<sup>2</sup>, Daokui Xu<sup>2</sup> and Barry C. Muddle<sup>2</sup>

<sup>1</sup>Southwest Aluminium (Group) Co. Ltd., CHALCO, Chongqing 401326, China

<sup>2</sup>ARC Centre of Excellence for Design in Light Metals, Monash University, VIC 3800, Australia

The dissolution and melting of constituent particles in a DC cast alloy 7150 during homogenisation has been investigated by means of differential scanning calorimetry, optical microscopy, scanning and transmission electron microscopy. It was found that the cast ingot contains particles of two predominant constituent intermetallic phases, namely  $\eta$  ( $\text{MgZn}_2(\text{Al,Cu})$ ) and S ( $\text{Al}_2\text{CuMg}$ ), together with small fractions of  $\text{Al}_7\text{Cu}_2\text{Fe}$  and  $\text{Mg}_2\text{Si}$  particles. During homogenisation treatments at temperatures between 440 and 470°C, all  $\eta$  phase particles can dissolve into the  $\alpha$ -Al matrix phase, and the dissolution process accelerates with increasing homogenisation temperature. Melting of the  $\eta$  and S phases commences at about 470°C and 481°C, respectively. To maximise the dissolution of both the  $\eta$  and S phases and to avoid overheating, a multi-step homogenisation process can be employed, which involves a first step homogenisation treatment at about 440-465°C to completely dissolve the lower melting point  $\eta$  phase, and a second homogenisation step at about 470-480°C to dissolve as much as possible of the higher melting point S phase.

**Keywords:** 7150; homogenisation; constituents; melting.

### 1. Introduction

Alloy 7150 is successfully used for key structural parts in aeronautical applications because of its potentially superior combination of high strength, toughness, fatigue durability and good corrosion resistance [1, 2]. It is known that segregation of alloying elements and constituent eutectic particles, existing in a large direct chill (DC) semi-continuously cast ingot, can decrease the hot workability in the hot forming process. An optimised homogenisation treatment is essential to remove the alloy element segregation, dissolve large soluble particles and form a fine and dense distribution of  $\text{Al}_3\text{Zr}$  dispersoids. The conventional homogenisation temperature for 7xxx alloys is below 470°C [3,4] to avoid an occurrence of overheating caused by local melting of low-melting point primary eutectic phases in the cast ingot. It has been reported that several different types of primary eutectic phases, such as S ( $\text{Al}_2\text{CuMg}$ ),  $\eta$  ( $\text{MgZn}_2$ ),  $\theta$  ( $\text{Al}_2\text{Cu}$ ), T ( $\text{Al}_2\text{Mg}_3\text{Zn}_3$  or  $\text{Al}_6\text{Mg}_{11}\text{Zn}_{11}$ ),  $\text{Mg}_2\text{Si}$ , and  $\text{Al}_7\text{Cu}_2\text{Fe}$ , can exist in cast Al-Zn-Mg-Cu alloys [5-7], and these phases can have different dissolution and/or melting temperatures. Therefore, a large volume fraction of primary eutectic particles would still remain in the 7xxx alloys after a conventional homogenisation treatment, and they might adversely affect the properties of the alloy.

This paper reports on the dissolution and melting of constituent particles, analysed by means of differential scanning calorimetry (DSC), optical microscopy, scanning electron microscopy (SEM) and transmission electron microscopy (TEM), in a DC-cast alloy 7150 under different homogenisation processes in the temperature range of 400-485°C. Dissolution and melting temperatures of different constituent particles, such as S and  $\eta$  phases, are identified. It is found that an improved ingot microstructure can be achieved by employing multi-step homogenisation processes. The mechanisms underpinning an optimised homogenisation process are also discussed.

## 2. Experimental Procedures

Samples were cut from near the centre of a CHALCO DC-cast alloy 7150 ingot (Al - 6.77Zn - 2.29Mg - 2.35Cu - 0.13Zr - 0.02Ti - 0.01Fe - 0.01Si, in wt.%). To study the thermal stability of the primary eutectic phases, samples were homogenised at temperatures from 400 to 485°C for up to 48 hours. To retain the microstructures as at the homogenisation temperatures, the homogenised samples were quenched immediately into warm water (~50°C) rather than cooling slowly in the furnace. Samples for reflected light microscopy and SEM examination were prepared by mechanical polishing. Thin foil specimens for TEM examination were punched from alloy sheets, ground to a thickness of 0.15 mm, and twin-jet electropolished at -25°C and 0.2A in a solution of 33% nitric acid and 67% methanol. Microstructural examination was performed using a Leica DMILM optical microscope, a JEOL 7001F SEM and a Philips CM20 TEM (200 kV). DSC analyses were carried out using a Perkin Elmer Diamond TG/DSC.

## 3. Results and Discussion

Figure 1 shows representative reflected light and back-scattered scanning electron (BSE) micrographs, energy dispersive x-ray spectra (EDXS) and electron microdiffraction patterns recorded from the as-cast 7150 samples. The microstructures of as-cast samples comprised  $\alpha$ -Al dendrites, primary eutectic intermetallic particles along dendrite boundaries and many finer precipitate particles within the dendrites, as shown in Figs. 1(a) and (b). It is evident from the BSE image in Fig. 1(b), that the intermetallic particles along the dendrite boundaries have two different contrasts. The EDX spectra recorded from the grey particles consistently indicated significant intensities attributable to Al, Cu and Mg, as shown in Fig. 1(c). Electron microdiffraction patterns recorded from these particles, such as Fig. 1(d), could be indexed consistently according to an orthorhombic structure of the S (Al<sub>2</sub>CuMg) phase (space group *Cmcm*,  $a = 0.400$  nm,  $c = 0.923$  nm,  $c = 0.714$  nm) [8]. Spectra from the bright particles revealed they contained Zn, Mg, Cu and Al, as shown in Fig. 1(e). Analysis of electron microdiffraction patterns recorded from these particles (Fig. 1(f)) indicated that it was an intermetallic phase that had a hexagonal structure identical to the  $\eta$  (MgZn<sub>2</sub>) phase (space group *P6<sub>3</sub>/mmc*,  $a = 0.5221$  nm,  $c = 0.8567$  nm) [9]. As Al has a similar atomic size to that of Mg and Cu has a similar atomic size to that of Zn, it appears very likely that some Mg atoms are substituted by Al atoms and some Cu atoms are substituted by Zn atoms in the  $\eta$  phase unit cell. It should also be mentioned that in the present study extensive electron microdiffraction analyses of the Zn-containing intermetallic particles has not found any body-centred cubic T phase (Al<sub>6</sub>Mg<sub>11</sub>Zn<sub>11</sub> with space group *Im $\bar{3}$* ,  $a = 1.416$  nm) [10]. In addition to the two predominant intermetallic phases, there were also small fractions of Al<sub>7</sub>Cu<sub>2</sub>Fe and Mg<sub>2</sub>Si particles detected in the as-cast microstructure and identified using the same techniques.

Figure 2 shows the changes in volume fraction of remaining constituent particles after homogenisation treatments at different temperatures from 425°C to 470°C for up to 48h. The dissolution process of constituent particles accelerated with an increase in homogenisation temperature, presumably primarily due to an increase in diffusion rate. At each temperature, the volume fraction approached a steady state after a certain time, typically in excess of 24h.

Figure 3 compares the reflected light micrographs and BSE images recorded from samples after homogenisation treatments for 48h at different temperatures. After homogenisation at 425°C for 48h, both interdendritic S and  $\eta$  phases were retained and the majority of precipitate particles within the dendrites had dissolved, Figs. 3(a) and (e). After homogenisation at 455°C for 48h, virtually all the  $\eta$  phase particles had dissolved and only some S phase and a small fraction of Al<sub>7</sub>Cu<sub>2</sub>Fe particles remained, Figs. 3(b) and (f). When the homogenisation temperature was increased to 470°C, Figs. 3(c) and (g), some S phase was still retained, but there was evidence of local melting, as revealed by numerous cavities or voids on the polished samples. At 485°C, almost all the S phase had disappeared and there were signs of significant local melting, as shown in Figs. 3(d) and (h). After homogenising

at 485°C, there was only a small fraction of intermetallic particles remaining and they were sparsely distributed. Spectra recorded from these remaining particles revealed that they contained Al, Cu and Fe, Fig. 3(i). Electron microdiffraction analyses indicated that they were an intermetallic phase with a tetragonal structure identical to the  $\text{Al}_7\text{Cu}_2\text{Fe}$  phase (space group  $P4/mnc$ ,  $a = 0.634$  nm,  $c = 1.487$  nm) [11], as shown in Fig. 3(j).

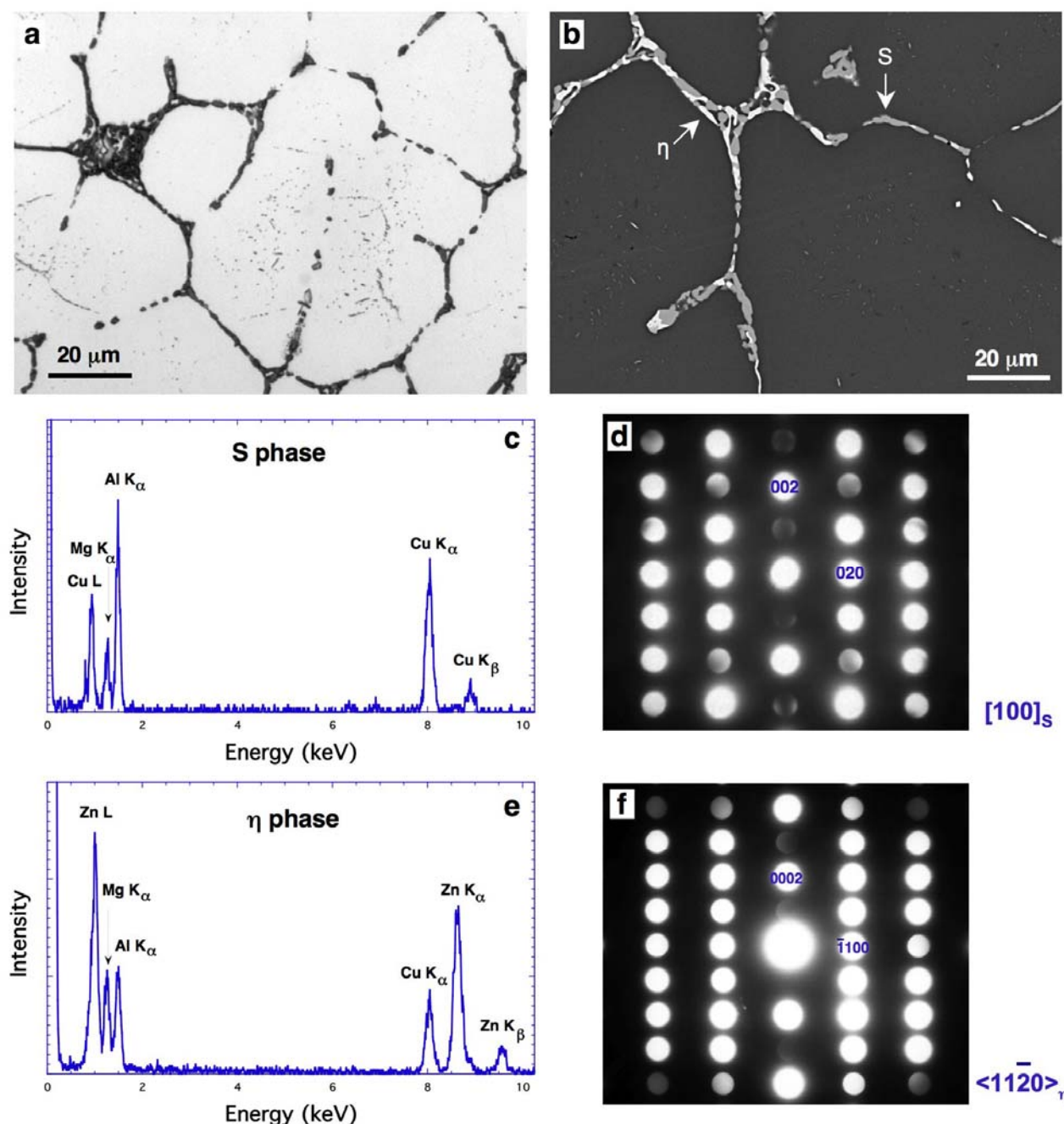


Fig. 1: (a) Reflected light and (b) BSE micrographs, respectively, of the as-cast alloy samples; (c) and (e) EDXS, and (d) and (f) electron microdiffraction patterns from the S and  $\eta$  phases, respectively.

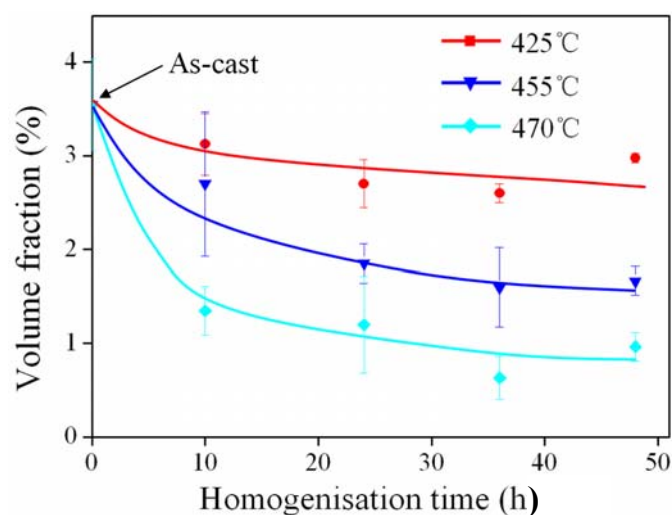


Fig. 2: Volume fraction changes of remaining intermetallic particles after homogenising for up to 48h at 425, 455 and 470°C, determined by image analysis from optical micrographs.

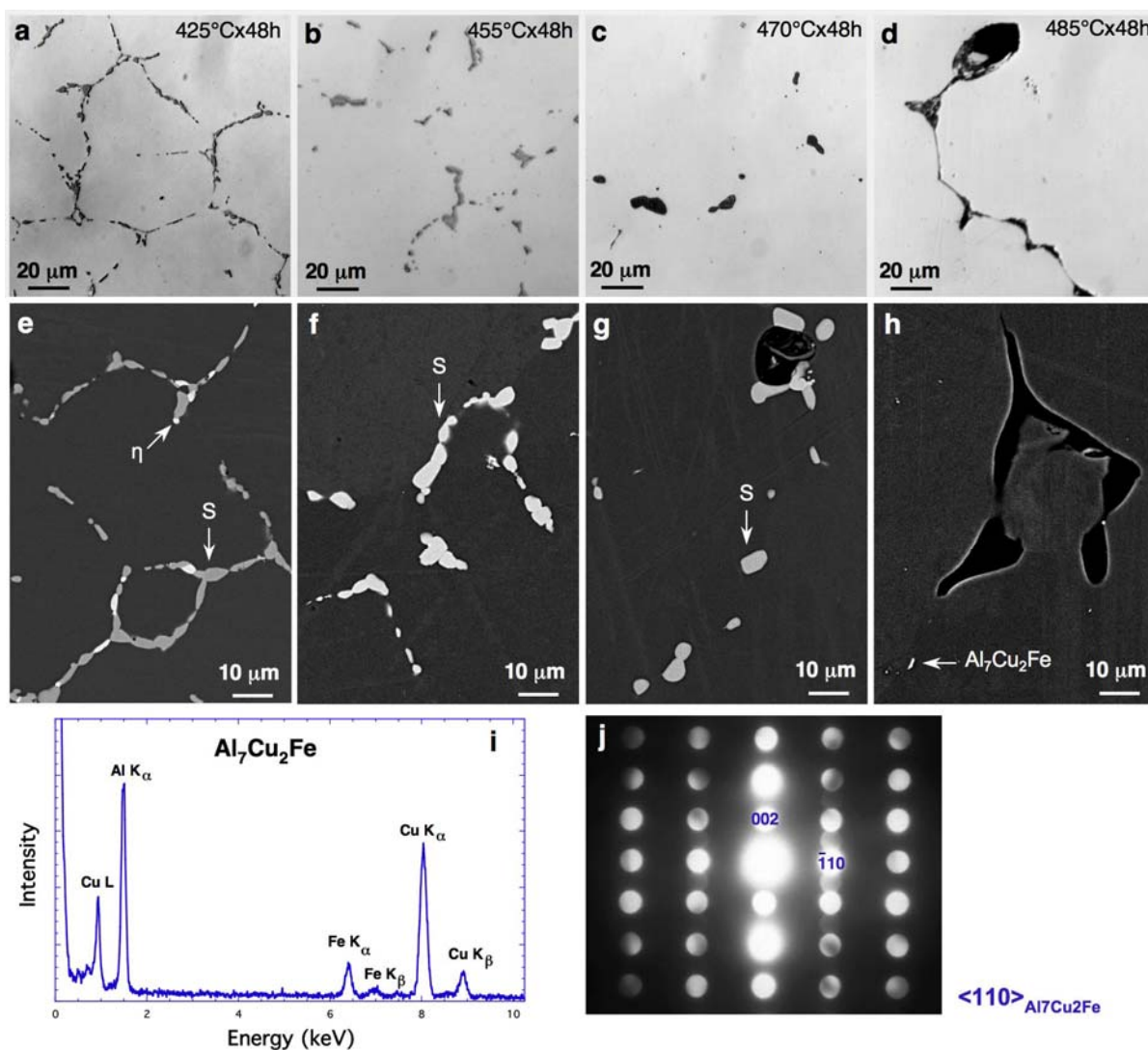


Fig. 3: Reflected light micrographs and BSE images of samples after homogenisation treatments of 48h at (a) and (e) 425°C, (b) and (f) 455°C, (c) and (g) 470°C, and (d) and (h) 485°C, along with (i) EDXS and (j)  $\langle 110 \rangle$  electron microdiffraction pattern recorded from the  $\text{Al}_7\text{Cu}_2\text{Fe}$  phase in (h).

DSC curves from as-cast and differently homogenised samples are presented in Fig. 4. There are two separate endothermic peaks in the as-cast condition and after homogenising for 48h at 400, 425 and 440°C. The onset of one peak is at about 470°C while that of the other peak is at about 481°C. In contrast, there is only one endothermic peak at 481°C for those samples homogenised at  $\geq 455^\circ\text{C}$ . In addition, the intensity of both peaks decreases with an increase in the homogenisation temperature. Based on the results shown in Figs. 1-3, it seems plausible to suggest that the peaks at 470°C and 481°C are associated with the melting of the  $\eta$  and S phases, respectively. When as-cast samples are homogenised at a temperature below 470°C, dissolution of both the  $\eta$  phase and some S phase takes place by solid-state diffusion into the  $\alpha$ -Al matrix. The  $\eta$  phase has been completely dissolved after homogenising for 48h at 455°C, Figs. 3(f) and 4.

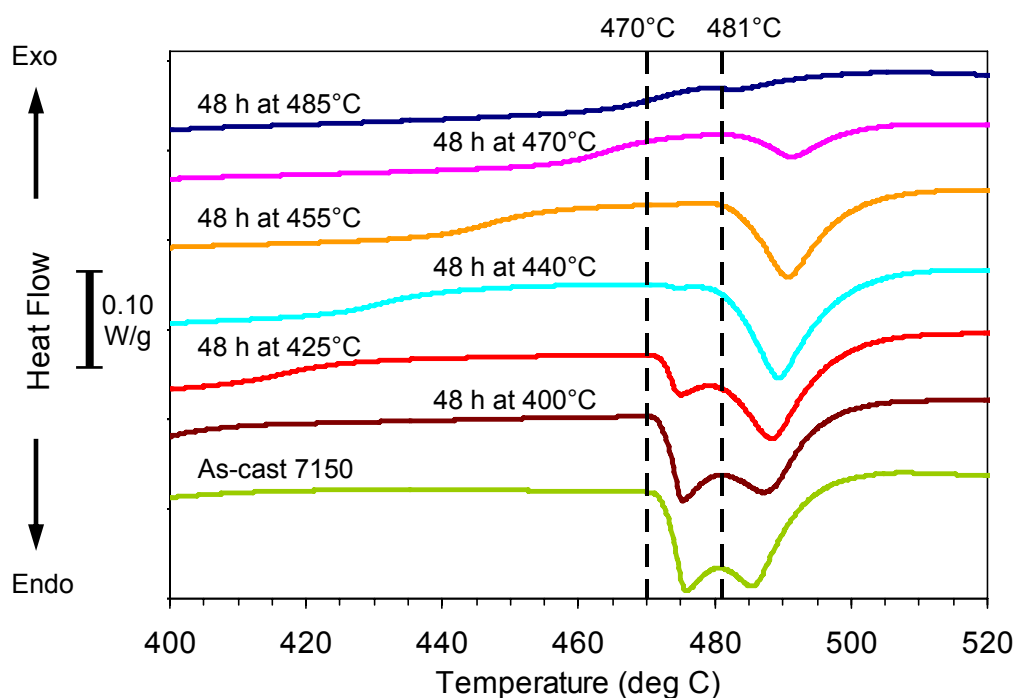


Fig. 4: DSC curves for alloy 7150 in the as-cast condition and after various homogenisation treatments (from 48h at 400°C to 48h at 485°C), at a DSC heating rate of 10°C/minute.

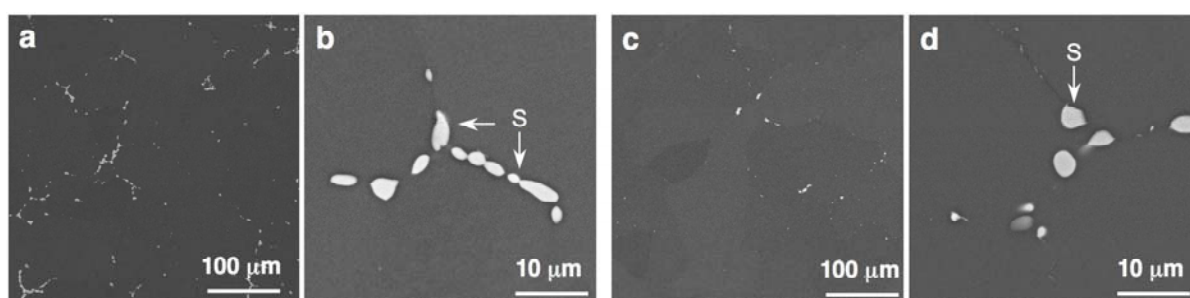


Fig. 5: BSE images of samples after homogenisation treatments of (a) and (b) 24h at 455°C, and (c) and (d) 24h at 455°C + 12h at 475°C, respectively.

To maximise the dissolution of both the  $\eta$  and S phases, it is suggested that a multi-step homogenisation process can be employed to alloy 7150 cast ingots, which involves a first step homogenisation treatment at below 470°C to dissolve the lower melting point  $\eta$  phase and a second step treatment at between 470-480°C to dissolve as much as possible of the higher melting point S phase while avoiding overheating. The optimisation of such a multi-step homogenisation process

requires a suitable combination of both temperature and time for both the first and the second step treatments. Based on the results shown above, it appears that the optimised temperature for the first step treatment might be at about 440-465°C and the optimised temperature for the second step treatment might be at 470-480°C. Fig. 5 presents BSE images of samples after two different homogenisation treatments. It shows clearly that it is possible to improve the dissolution of constituent particles by a two-step homogenisation treatment. After the first homogenisation step at 455°C for 24h, virtually all the  $\eta$  phase particles had dissolved and only some S phase and a very small fraction of  $\text{Al}_7\text{Cu}_2\text{Fe}$  particles remained, Figs. 5(a) and (b). After the second homogenisation step at 475°C for 12h, some S phase was still retained but there was a reduction in the volume fraction of S phase particles to a level of about 0.5% (determined by image analysis from reflected light micrographs) without any obvious signs of overheating, Figs. 5(c) and (d). The risk of overheating will be even lower if ingots are heated slowly in a circulating air furnace, compared to the very rapid heating rates achieved with the small samples immersed in salt baths in the present work. It should also be mentioned that care must also be taken to ensure an optimum size-distribution of Zr-containing dispersoids when designing an optimised two-step homogenisation treatment. More detailed analyses of two-step homogenisation treatments are required to investigate this.

#### 4. Summary

DC-cast alloy 7150 ingots contain two predominant types of constituent intermetallic particles:  $\eta$  ( $\text{MgZn}_2(\text{Al,Cu})$ ) and S ( $\text{Al}_2\text{CuMg}$ ) phases. A small amount of  $\text{Al}_7\text{Cu}_2\text{Fe}$  and  $\text{Mg}_2\text{Si}$  particles are also observed. During homogenisation for 48h between 440 and 470°C, all  $\eta$  and some S phase dissolves by solid state diffusion into the  $\alpha$ -Al matrix, and the dissolution process accelerates with an increase in homogenisation temperature. Melting of the  $\eta$  and S phases commences at about 470°C and 481°C, respectively. To maximise the dissolution of both  $\eta$  and S phases and to avoid overheating, a multi-step homogenisation process can be employed. This involves a first step homogenisation treatment at about 440-465°C to dissolve the lower melting point  $\eta$  phase, followed by a second step treatment at about 470-480°C to dissolve as much as possible of the higher melting point S phase.

#### Acknowledgements

The authors would like to thank the Aluminium Corporation of China (CHALCO) for supporting this work financially and providing materials as part of the Australia-China International Centre for Light Alloys Research (ICLAR).

#### References

- [1] I.J. Polmear: *Light Alloys*, 4<sup>th</sup> ed., Oxford; Burlington, MA: Elsevier/Butterworth-Heinemann, 2006.
- [2] E.A. Starke Jr and J.T. Staley: *Prog. Aerospace Sci.* 32 (1995) 131.
- [3] N. Q. Chinh, Z. S. Kovács, L. Reich, F. Székely, J. Illy and J. Lendvai: *Materials Science Forum* 217/222 (1996) 1293–1298.
- [4] Y. Hideo and B. Yoshio: *J. Japan Inst. Light Metals* 31 (1981) 20–29.
- [5] C. Mondal and A. K. Mukhopadhyay: *Mater. Sci. Eng.* 391A (2005) 367–376.
- [6] S.T. Lim, Y.Y. Lee, and I.S. Eun: *Mater. Sci. Forum* 519–521 (2006) 549–554.
- [7] L.L. Rokhlin, T.V. Dobatkina, N.R. Bochvar, and E.V. Lysova: *J. Alloys Compd.* 367 (2004) 10–16.
- [8] H. Perlitz, A. Westgren and *Arkiv Foer Kemi: Min. Och Geologi*, 16B (1943) 1-5.
- [9] Y. Komura and K. Tokunaga: *Acta Crystallogr.* 36B (1980) 1548.
- [10] G. Bergman, J.L.T. Waugh and L. Pauling: *Acta Crystallogr.* 10 (1957) 254-259.
- [11] M.G. Bown and P.J. Brown: *Acta Crystallogr.* 9 (1956) 911-914.